Biochemical Pharmacology 82 (2011) 1781–1791

Contents lists available at ScienceDirect

Biochemical Pharmacology

journal homepage: www.elsevier.com/locate/biochempharm

Indomethacin induces cellular morphological change and migration via epithelial-mesenchymal transition in A549 human lung cancer cells: A novel cyclooxygenase-inhibition-independent effect

Tomoko Kato [a], Hiromichi Fujino [a,*], Satomi Oyama [a], Tatsuo Kawashima [b], Toshihiko Murayama [a]

[a] Laboratory of Chemical Pharmacology, Graduate School of Pharmaceutical Sciences, Chiba University, 1-8-1 Inohana, Chuo-ku, Chiba 260-8675, Japan
[b] Department of Internal Medicine, Toho University School of Medicine, Sakura Hospital, Sakura 285-8741, Japan

ARTICLE INFO

Article history:
Received 6 June 2011
Accepted 27 July 2011
Available online 4 August 2011

Keywords:
Indomethacin
EMT
E-cadherin
MMP-9
NSCLC

ABSTRACT

Levels of cyclooxygenase (COX)-2 and its metabolite prostaglandin E_2 (PGE_2) are frequently increased in colon cancer and other cancers including lung cancer. Non-steroidal anti-inflammatory drugs are considered to have chemo-preventive effects on these diseases by reducing the biosynthesis of PGE_2 via their inhibition of COX-2. Although the COX-2/PGE_2 pathway may directly impact on lung carcinogenesis, some population-based cohort studies of NSAIDs showed no significant protective effects. In this study, using human non-small-cell lung cancer A549 cells, we examined the effects of indomethacin, a potent NSAID, on the growth and motility of lung cancer cells. Besides inhibiting PGE_2 production and cellular growth, indomethacin caused drastic morphological changes with a loss of stress fibers in a time- and dose-dependent manner. Interestingly, the change in cellular shape caused by indomethacin was not seen when the cells were treated with aspirin or diclofenac, two other NSAIDs, despite the concentrations used being sufficient to inhibit PGE_2 production. The indomethacin-induced morphological changes in A549 cells were accompanied by a reduction in levels of the adhesion molecule E-cadherin and a component of basal lamina, collagen IV, as well as an increase in the activity of a collagenase, matrix metalloprotease-9. Furthermore, indomethacin-induced shape changes resulted in enhanced motility via regulation of peroxisome proliferator-activated receptor γ. The dual effects of indomethacin, inhibition of cellular growth and enhancement of migration, would explain, to some extent, the difficulty in using this NSAID for lung cancer therapy.

1. Introduction

1.1. Cyclooxygenase, cellular motility, and epithelial-mesenchymal transition

Preventive effects against mammary carcinomas and in cancer cell lines suggest that non-steroidal anti-inflammatory drugs (NSAIDs) are potential chemo-protective agents for colon, esophageal, ovarian, stomach, breast, pancreatic, and lung cancers [1,2]. NSAIDs are widely believed to inhibit cyclooxygenase (COX)-2 and/or COX-1 followed by the biosynthesis of prostanoids such as prostaglandin E_2 (PGE_2). Increased levels of PGE_2 following the overexpression of COX-2 have been well documented in the regulation of cancer development as well as metastasis [3]. Metastasis causes almost 90% of cancer-related deaths; however, its pathogenesis is poorly understood because the induction of tumor metastasis is a multi-step process [4,5]. However, in some cancer cells, metastasis may be initiated by the untying of tightly bound neighboring cells and by the stripping of the underlying basement membranes from the cells, by which the cells acquire the ability to migrate. These cellular phenomena are known as the epithelial-mesenchymal transition (EMT) and characterized by a loss of cellular adhesion and an increase in cellular motility, which play important roles in early embryonic morphogenesis as well as tissue repair processes including wound healing [6,7]. The loss of cellular adhesion with EMT is well characterized at the molecular level by a down-regulation of the cell surface expression of E-cadherin, an adhesion molecule that contributes to the tight homotypic interaction between the cells [6–8]. Another common feature of EMT is an increase in the expression of matrix metalloproteinase (MMP)-2 and/or -9, which play critical roles in the loss of basal-apical polarity through proteolytic degradation of components of basement membranes such as collagen IV, elastin, and α1-antitrypsin [7,9–11]. Thus, during wound healing, EMT allows epithelial cells to

Abbreviations: NSAIDs, non-steroidal anti-inflammatory drugs; COX, cyclooxygenase; PGE_2, prostaglandin E_2; EMT, epithelial-mesenchymal transition; MMP, matrix metalloproteinase; NSCLC, non-small-cell lung cancer; EGFR, epidermal growth factor receptor; PPAR, peroxisome proliferator-activated receptor; MET, mesenchymal-epithelial transition.

* Corresponding author. Tel.: +81 43 226 2875; fax: +81 43 226 2875.
E-mail address: fujino@p.chiba-u.ac.jp (H. Fujino).

0006-2952/$ – see front matter © 2011 Elsevier Inc. All rights reserved.
doi:10.1016/j.bcp.2011.07.096

migrate to the site of injury by freeing them from homotypic adhesion and the basement membrane as a mesenchymal phenotype. Therefore, the loss of E-cadherin and increased activity of MMP-2 or -9 are good predictors of poor prognosis in cancer patients since these changes caused by EMT promote the migration and invasion of cancer cells, namely metastasis [8,12,13].

1.2. Lung cancer, chemotherapy, and metastasis

Lung cancer is the leading cause of cancer-related death around the world, with approximately 85–90% of cases involving non-small-cell lung cancer (NSCLC) [14,15]. One common complication of NSCLC is metastasis to the brain, responsible for significant increases in morbidity and motility [16,17]. The most common treatment for NSCLC is platinum-based chemotherapy; however, the survival benefit remains less than 30% of patients with metastatic cancer [14]. Agents have been developed that target the epidermal growth factor receptor (EGFR), since this receptor is activated in more than half of patients with NSCLC [14]. However, these EGFR-tyrosine kinase inhibitors produce durable responses against brain metastasis in some patients with NSCLC [18]. On the other hand, preclinical and clinical studies indicate increased levels of COX-2 and its metabolite PGE_2 to be associated with enhanced metastatic potential in NSCLC [19]. Indeed, over-expression of COX-2 was reported in approximately 70% of lung adeno-carcinomas [20]. Although the mechanisms responsible for the elevated COX-2 levels in lung cancer are not fully understood, COX-2 inhibitors including NSAIDs are believed to prevent lung cancer since COX-2/PGE_2 may directly impact lung carcinogenesis and metastasis. Thus, regular use of NSAIDs including indomethacin has been associated with an approximately 61–68% reduction in the risk of lung cancer in some epidemiological studies [21]. However, despite basic studies elucidating that the COX-2/PGE_2 pathway is involved in lung cancer development and metastasis, including NSCLC, some population-based cohort studies of NSAIDs showed no significant protective effects [22,23]. However, these studies had significant limitations. Most patients in the Medicaid population tend to use not costly over-the-counter NSAIDs but rather free prescription NSAIDs [22]. Moreover, no information was provided about the use of non-prescription NSAIDs such as ibuprofen, or compliance [22]. Therefore, there is a need for detailed information on the effect of individual NSAIDs on lung cancer, since these studies bundled NSAIDs together. In this study, we have examined the effects of indomethacin on lung cancer in a COX-2-expressing human NSCLC line, A549 cells. Besides inhibiting the production of PGE_2 and cellular growth, indomethaicin but not aspirin or diclofenac, enhanced cellular migration in a manner independent of COX inhibition. Thus, indomethacin shows dual counteracting effects on NSCLC, which would explain, to some extent, the difficulty in using this NSAID for lung cancer therapy.

2. Materials and methods

2.1. Cell culture and materials

A549 human lung cancer cells were cultured at 37 °C with 5% CO_2/95% air and in Dulbecco's modified Eagle's medium (Sigma, St. Louis, MO) containing 10% fetal bovine serum (Thermo Scientific, Waltham, MA), 100 IU/ml penicillin (Meiji Seika, Tokyo, Japan), and 100 μg/ml streptomycin (Meiji Seika, Tokyo, Japan). All materials were obtained from Wako Pure Chemical (Osaka, Japan) unless stated otherwise.

2.2. Phalloidin staining of actin stress fibers and imaging

Approximately 3×10^5 cells were grown for 24 h in each wells of 6-well plates with glass cover-slips and then, 16 h prior to the experiments, switched from their regular culture medium to Opti-MEM (Invitrogen, Carlsbad, CA) containing 100 IU/ml penicillin and 100 μg/ml streptomycin. Cells were treated with either vehicle (dimethyl sulfoxide) or 300 μM indomethacin (Sigma, St. Louis, MO), 3 mM aspirin (acetylsalicylic acid), 300 μM diclofenac, 1 μM PGE_2 (Cayman, Ann Arbor, MI), or 10 μM troglitazone (Cayman, Ann Arbor, MI) for 0–16 h. Cells were then fixed for 15 min in 4% paraformaldehyde in 1× phosphate-buffered saline, quenched 3 times for 10 min in 0.1 M glycine (pH 7.4), and permeabilized for 15 min in 2× SCC (30 mM NaCl, 300 mM sodium citrate) containing 0.1% (v/v) Triton-X 100 (Sigma, St. Louis, MO) as described previously [24]. The cells were stained with TRITC-conjugated phalloidin (Sigma, St. Louis, MO), and visualized with a laser-scanning confocal microscope (Olympus, Tokyo, Japan) using optical band filters for Texas Red and visible wavelengths.

2.3. Prostaglandin E_2 enzyme immunoassay

Cells were cultured in 6-well plates and the medium was replaced with fresh Opti-MEM containing 100 IU/ml penicillin and 100 μg/ml streptomycin. Cells were then treated with either vehicle or 300 μM indomethacin (Sigma, St. Louis, MO), 3 μM aspirin, and 300 μM diclofenac for 16 h. The quantitative determination of PGE_2 concentrations in the cell culture supernatants was carried out by enzyme immunoassay according to the manufacturer's instructions (Cayman, Ann Arbor, MI). Optical density was determined using a microplate reader with a SUNRISE rainbowfilter (TECAN, Mannedorf, Switzerland) at 405 nm. The amount of endogenous PGE_2 in vehicle-treated control cells was approximately 100 pg/ml to 200 pg/ml. Data were normalized to the amount of PGE_2 in vehicle-treated cells as 100%.

2.4. Wound-healing assay

Cells were grown in 6-well plates to confluence and formed a monolayer covering the surface of the entire plate. Wounds were created with a pipette tip as described previously [25]. Cells were then treated with either vehicle or 300 μM indomethacin (Sigma, St. Louis, MO) for approximately 24 h or 48 h at 37 °C. The wounds were assessed by comparing the 0 and 24 h or 48 h micrographs at several marked points along with the wounded area in each well. Plates were examined by phase contrast microscopy using a Nikon Diaphot microscope (Nikon, Tokyo, Japan) and images were obtained using a Nikon D70 digital camera (Nikon, Tokyo, Japan) and processed using Nikon Capture 4 (Nikon, Tokyo, Japan).

2.5. Cell migration assay

Approximately 3×10^3 cells were seeded on Costar Transwell (#3422, Corning, New York, NY) 24-well insets (6.5 mm in diameter) with 8 μm pores in 100 μl of medium in their upper chambers and 600 μl in the lower chambers. Cells were grown for 4 days and the medium was replaced with Opti-MEM containing 100 IU/ml penicillin and 100 μg/ml streptomycin at 100 μl and 600 μl in the upper and lower chambers, respectively. Cells were then treated with either vehicle or 300 μM indomethacin (Sigma, St. Louis, MO) for 24 h or 48 h at 37 °C. Cells that had migrated through the filter membrane to the lower chamber were trypsinized and counted under a Nikon eclipse TS100 microscope (Nikon, Tokyo, Japan) as described previously [25]. In the case of troglitazone treatment, cells were pretreated with either vehicle or 10 μM troglitazone (Cayman, Ann Arbor, MI) for 15 min prior to the treatment with 300 μM indomethacin.

2.6. Cell counts and viability

Approximately 1×10^5 cells were seeded on 6-well plates for 24 h and the medium was replaced with Opti-MEM containing 100 IU/ml penicillin and 100 μg/ml streptomycin. Cells were treated with either vehicle or 300 μM indomethacin (Sigma, St. Louis, MO) for 24 h or 48 h at 37 °C. Cells were then trypsinized and counted under a Nikon eclipse TS100 microscope (Nikon, Tokyo, Japan). Cell viability is expressed as the number of viable cells counted using 0.3% (w/v) trypan blue dye (Sigma, St. Louis, MO).

2.7. Western blotting

Cells were cultured in 6-well plates and the medium was replaced with fresh Opti-MEM containing 100 IU/ml penicillin and 100 μg/ml streptomycin prior to the immunoblotting experiments. Cells were then treated with 300 μM indomethacin (Sigma, St. Louis, MO) for the periods indicated in the figures at 37 °C. In the experiments using troglitazone, cells were pretreated with either vehicle or 10 μM troglitazone (Cayman, Ann Arbor, MI) for 15 min at 37 °C, and then treated with either vehicle or 300 μM indomethacin for 8 h. Cells were scraped into a lysis buffer consisting of 150 mM NaCl, 50 mM Tris–HCl (pH 8.0), 5 mM EDTA (pH 8.0), 1% Igepal CA-630 (MP Biomedicals, Aurora, OH), 0.5% sodium deoxycholate, 10 mM sodium fluoride, 10 mM disodium pyrophosphate, 0.1% SDS, 0.1 mM phenylmethylsulfonyl fluoride, 1 mM sodium orthovanadate, 10 μg/ml leupeptin (Sigma, St. Louis, MO), and 10 μg/ml aprotinin and transferred to microcentrifuge tubes. The samples were rotated for 30 min at 4 °C and centrifuged at 16,000 × *g* for 15 min. For the detection of E-cadherin and EGFR, cells were scraped and sonicated in a lysis buffer consisting of 20 mM Tris–HCl (pH 7.5), 10 mM EDTA (pH 8.0), 2 mM EGTA, 2 mM phenylmethylsulfonyl fluoride, 2 mM sodium orthovanadate, 100 μg/ml leupeptin, and 10 μg/ml aprotinin. The samples were centrifuged at 16,000 × *g* for 15 min at 4 °C, the supernatant (cytosolic fraction) was removed, and the pellet (particulate fraction) was solubilized with lysis buffer containing 0.2% Triton X-100 (Sigma, St. Louis, MO) again to remove insoluble debris. Aliquots of sample containing approximately 80 μg of protein were electrophoresed on 10% SDS-polyacrylamide gels and transferred to nitrocellulose membranes as described previously [26]. The membranes were incubated for 16 h at 4 °C in 3% non-fat milk for the detection of E-cadherin, EGFR, and collagen IV or in 1% non-fat milk for the detection of β-tubulin. Incubations were carried out for 2–3 h at room temperature in 3% non-fat milk containing a 1:1000 dilution of anti-E-cadherin antibody (610182, BD Transduction Laboratories, San Jose, CA); a 1:1000 dilution of anti-collagen IV antibody (ab6586, Abcam, Cambridge, UK) in 5% bovine serum albumin (BSA, Sigma, St. Louis, MO); a 1:1000 dilution of anti-EGFR antibody (sc-003, Santa Cruz Biotechnology, Santa Cruz, CA) in 1% non-fat milk; or a 1:1000 dilution of anti-β-tubulin antibody (T4026, Sigma, St Louis, MO) in 3% BSA. After incubating with primary antibodies, membranes were washed twice and incubated for 1 h at room temperature with a 1:4000 dilution of the appropriate secondary antibodies conjugated with horseradish peroxidase as described previously [25]. After washing twice, immunoreactivity was detected and visualized with a chemi-luminescence imaging system, LAS-1000 (Fuji Film, Tokyo, Japan). To ensure equal loading of proteins, the membranes were stripped and re-probed with anti-EGFR antibody or anti-β-tubulin antibody under the conditions described above.

2.8. Gelatin zymography

Cells were cultured in 6 cm dishes and the medium was replaced with fresh Opti-MEM containing 100 IU/ml penicillin and 100 μg/ml streptomycin prior to the experiments. Cells were treated with 300 μM indomethacin (Sigma, St. Louis, MO) for the periods indicated in the figure, or 0–300 μM indomethacin for 16 h at 37 °C. In the experiments using troglitazone, cells were pretreated with either vehicle or 10 μM troglitazone (Cayman, Ann Arbor, MI) for 15 min at 37 °C and then treated with either vehicle or 300 μM indomethacin for 8 h. Samples of 3 ml of the supernatants of culture medium were collected and precipitated with 3 ml of 20% trichloroacetic acid (Sigma, St. Louis, MO) in ice-cold acetone for 16 h at −20 °C. The samples were mixed with 10 ml of ice-cold acetone and incubated for 16 h at −20 °C. They were then centrifuged at 10,000 × *g* for 15 min at 4 °C. The pellets were washed with 3 ml of diethyl ether and centrifuged at 10,000 × *g* for 15 min at 4 °C. The pellets were dissolved with 40 μl of sample buffer consisting of 62.5 mM Tris–HCl (pH 6.8), 10% glycerol, 2% SDS, and a trace amount of bromophenol blue. Samples were loaded under non-denaturing conditions into 10% polyacrylamide gels supplemented with 0.2% gelatin (Sigma, St. Louis, MO). After electrophoresis, gels were incubated in renaturing buffer containing 2.5% Triton X-100 (Sigma, St. Louis, MO) in water for 30 min at room temperature with gentle agitation, and then equilibrated in developing buffer consisting of 50 mM Tris–HCl (pH 7.5), 0.2 M NaCl, 5 mM $CaCl_2$, and 0.2% Tween 20 (Sigma, St. Louis, MO) for 30 min at room temperature with gentle agitation. Gels were incubated in developing buffer at 37 °C for 16 h and stained with 0.5% Coomassie Blue R-250 (Eastman Kodak, Rochester, NY) in destaining solution (methanol:acetic acid:-water = 5:1:4). After destaining, each individual band on the gel was measured for both size and intensity by scanning densitometry using NIH image, to provide a quantitative assay of the enzymatic activity of MMP-9.

3. Results

3.1. Indomethacin induces cellular morphological changes in A549 cells

To examine the effect of indomethacin on the cellular cytoskeleton, the human adenocarcinomic alveolar epithelial line A549 cells were treated with 300 μM indomethacin for up to 16 h. As shown in the upper panels of Fig. 1, the phalloidin-stained cells showed the formation of stress fibers at time 0. However, treatment with indomethacin gradually induced cellular morphological changes. Thus, the A549 cells shrank, elongated, and dissociated in a time-dependent manner with the treatment with indomethacin. These morphological changes were accompanied by a loss of actin stress fibers. To determine if the cellular changes and loss of stress fibers were indomethacin-specific phenomena, the effects of other typical NSAIDs were examined. As shown in Fig. 2A, treatment with 300 μM indomethacin for 16 h, again, clearly induced morphological changes and a loss of stress fibers. However, treatment with 3 mM aspirin, 300 μM diclofenac, or 300 μM sulindac (data not shown) for 16 h did not have these effects. Interestingly, the indomethacin-induced morphological changes in A549 cells were reversible. Thus, after washing and the removal of indomethacin for 16 h, cells returned to their original shape, as shown in Fig. 1 (data not shown).

3.2. Indomethacin-induced morphological changes could be cyclooxygenease/prostaglandin E_2-independent effects

To confirm if the ineffectiveness of the NSAIDs examined, with the exception of indomethacin, on cellular morphological changes was due to the concentrations used, the amount of PGE_2 was measured, since A549 cells were reported to express endogenous COX-2 [27]. As described in Section 2.3, the amount of endogenous

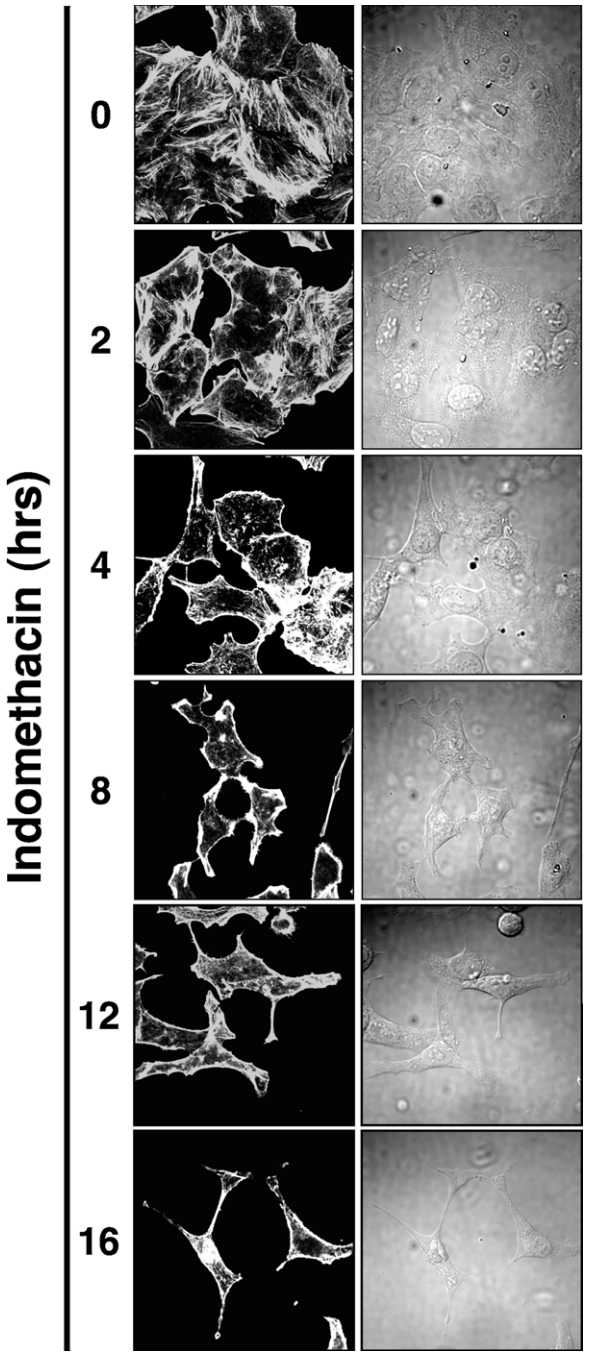

Fig. 1. Effect of indomethacin on the formation of actin stress fibers and cellular morphology. A549 cells were treated with either vehicle or 300 μM indomethacin for the periods indicated and were stained with TRITC-phalloidin to examine the changes in the formation of stress fibers. Images were obtained as described under Section 2. Left panels: images of TRITC-phalloidin-stained stress fibers in indomethacin-treated A549 cells. Right panels: the same fields as shown in the left panels photographed under visible light. The results are representative of more than three independent experiments.

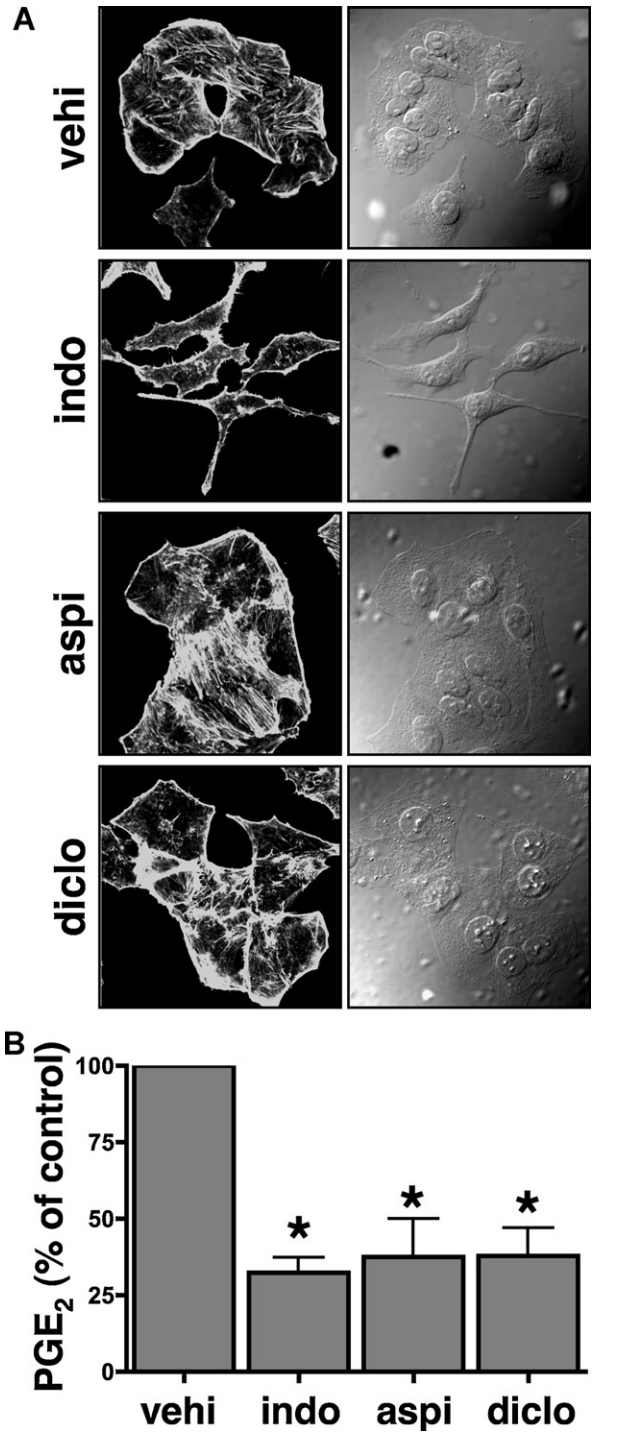

Fig. 2. Effects of NSAIDs on the formation of actin stress fibers and inhibition of PGE_2 production. A549 cells treated with either vehicle or 300 μM indomethacin, 3 mM aspirin, and 300 μM diclofenac for 16 h were stained with TRITC-phalloidin (A), and subjected to measurements of the amount of PGE_2 produced (B). A: Left panels: images of TRITC-phalloidin-stained stress fibers in indomethacin-treated A549 cells. Right panels: the same fields as shown in the left panels photographed under visible light. Images are representative of three independent experiments. B: PGE_2 enzyme immunoassay data are normalized to endogenous PGE_2 production and are the means ± S.D. for three independent experiments. $^*p < 0.05$, analysis of variance, as compared with vehicle treatment.

PGE_2 in vehicle-treated control cells was approximately 100 pg/ml to 200 pg/ml. As shown in Fig. 2B, treatment of the cells with 3 mM aspirin, 300 μM diclofenac, and 300 μM sulindac (data not shown) as well as 300 μM indomethacin for 16 h significantly reduced the amount of PGE_2 by approximately 70%, to 30% of control. Thus, the concentrations of NSAIDs examined were sufficient to inhibit the production of PGE_2, *i.e.*, were sufficient to inhibit COX activity. To confirm if the morphological changes and a loss of stress fibers were due to the decrease in the formation of PGE_2 by indomethacin, we treated the cells with exogenous PGE_2 and indomethacin to see if these effects of indomethacin were restored. As shown in Fig. 3, concomitant treatment with exogenous 1 μM PGE_2 altered neither the indomethacin-induced cellular changes nor a loss of stress fibers. These results suggest that inhibition of COX activity

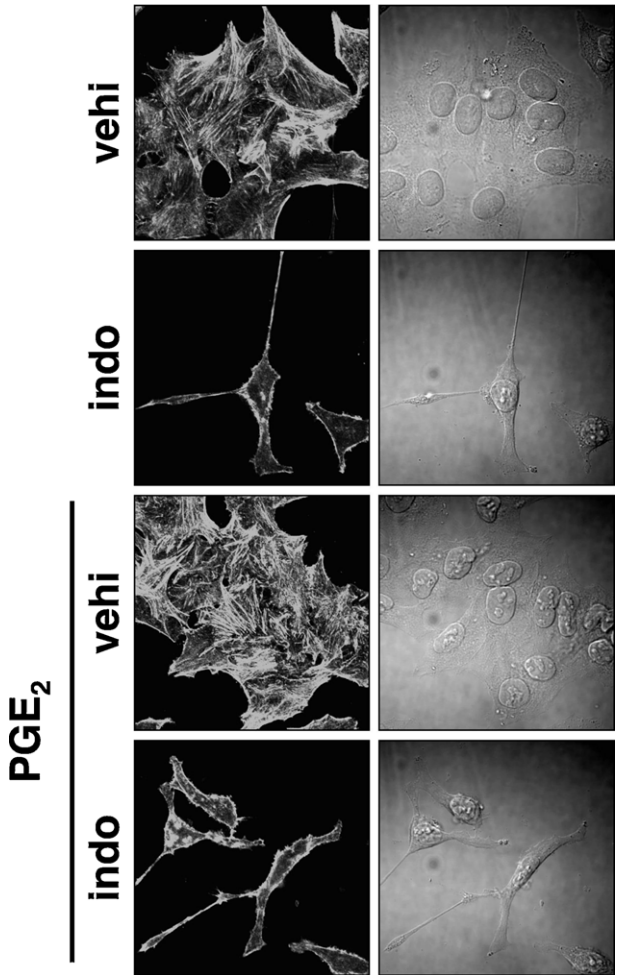

Fig. 3. Effect of PGE_2 on the indomethacin-induced reduction of stress fibers and changes in cellular morphology. A549 cells were treated with vehicle or 300 μM indomethacin concomitantly with either vehicle or 1 μM PGE_2 for 16 h and stained with TRITC-phalloidin. Left panels: images of TRITC-phalloidin-stained stress fibers in indomethacin-treated A549 cells. Right panels: the same fields photographed under visible light. Images are representative of three independent experiments.

by NSAIDs is not sufficient and/or required for induction of the cellular morphological changes and a loss of stress fibers by indomethacin treatment.

3.3. Indomethacin enhances cellular migration but not cellular growth in A549 cells

The reorganization of the cellular cytoskeleton and extracellular matrix has been implicated in the regulation of cancer cell migration and metastasis [4,28,29]. Therefore, the potential for the A549 cells to migrate after indomethacin treatment was examined using a wound-healing assay. Confluent cells were scratched using a pipette tip to create wounds and wound closure was evaluated following indomethacin treatment for 1 and 2 days. As shown in Fig. 4A, in vehicle-treated control cells, time-dependent closure was seen from both sides of the wound, whereas indomethacin-treated cells were spread out across the wound. Using Transwell filters [25], we further examined the ability of A549 cells to migrate. As shown in Fig. 4B, approximately 5 times more cells migrated from the upper to lower chambers following treatment with indomethacin for 1 day compared with vehicle-treated cells. Interestingly, on day 2, the control cells showed a linear rate of migration. However, in the indomethacin-treated cells, the migration rate was decreased and the curve was parabolic. We

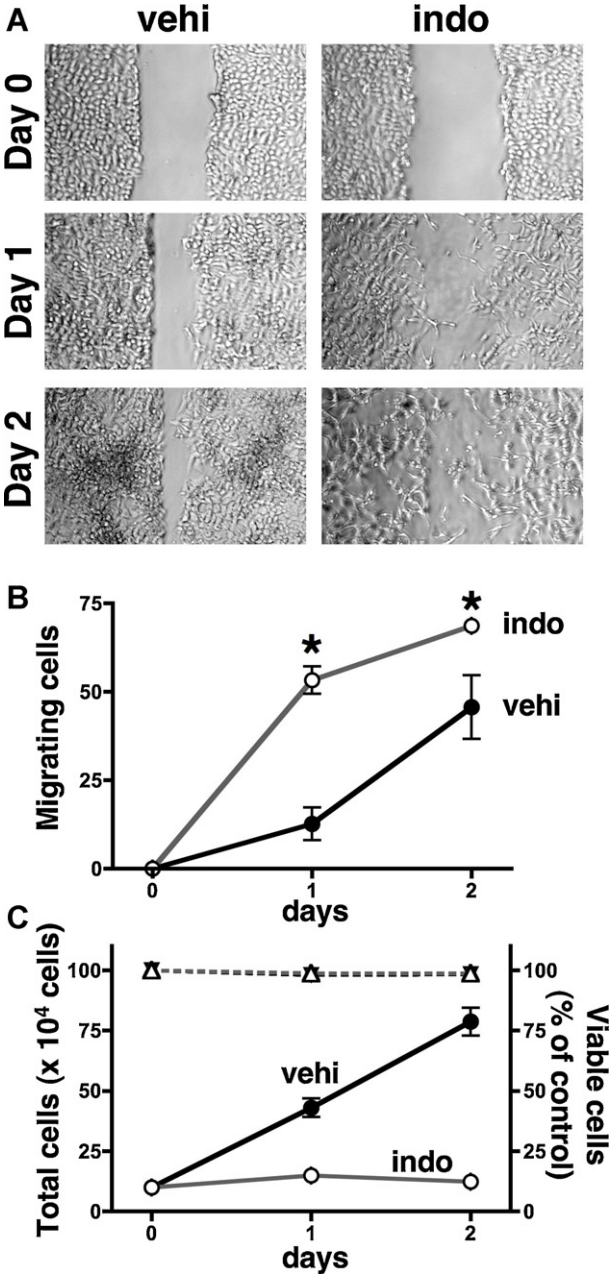

Fig. 4. Effects of indomethacin on cell migration in a wound-healing assay (A) and in a transwell filter assay (B), and on cell growth as well as cellular toxicity (C). A: Wounds were made in confluent cell layers, then cells were treated with either vehicle or 300 μM indomethacin for the periods indicated. Images are representative of three independent experiments and were obtained as described under Section 2. B: A549 cells in the upper chamber were treated with vehicle or 300 μM indomethacin for the periods indicated. The cells that had migrated to the bottom chamber after the periods indicated were trypsinized and then counted. The line plot represents the migrating cells after the periods indicated (mean ± S.E.M.) from three independent experiments. C: A549 cells were treated with vehicle or 300 μM indomethacin for the periods indicated. Cells were then counted (left *Y*-axis, solid lines; ●, vehicle; ○, indomethacin) or ratios of viable cells were estimated by using trypan blue staining (right *Y*-axis, dashed lines; ▼, vehicle; △, indomethacin) as described under Section 2. Data are normalized to the vehicle-treated controls (0 h) as 100%. $^*p < 0.05$, analysis of variance, as compared with vehicle treatment.

therefore examined the growth rates of the indomethacin-treated A549 cells compared with the vehicle-treated control cells. As shown in Fig. 4C left *Y*-axis, the vehicle-treated control cells showed a linear growth rate. For the indomethacin-treated cells, the number of cells counted was not altered after indomethacin

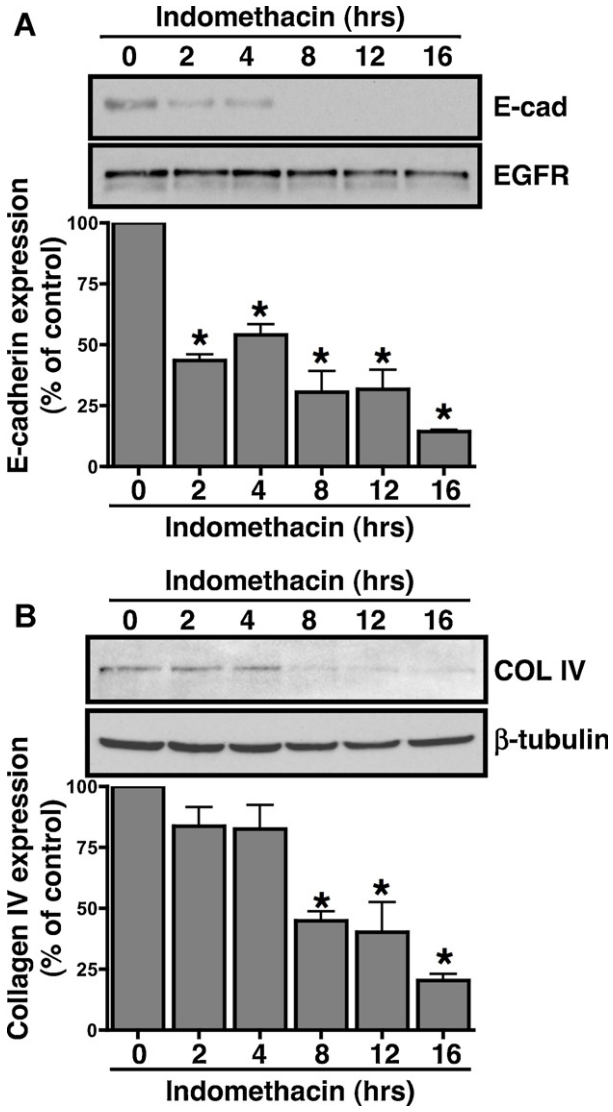

Fig. 5. Effects of indomethacin on cellular surface expression of E-cadherin or collagen IV. A549 cells were treated with vehicle or 300 μM indomethacin for the periods indicated. A: A particulate (membrane) fraction was prepared as described under Section 2 and subjected to immunoblot analysis for E-cadherin (E-cad, upper panel) and EGF receptors (EGFR, lower panel). A representative immunoblot is shown. The histogram represents the ratio of E-cadherin to EGFR as assessed with pooled densitometric data (mean ± S.D.) from three independent experiments. B: Upper panel: immunoblotting with antibodies against collagen IV (COL IV). Lower panel: immunoblotting with antibodies against β-tubulin. The histogram represents the ratio of collagen IV to β-tubulin as assessed with pooled densitometric data (mean ± S.D.) from three independent experiments. Data are normalized to the vehicle-treated controls (0 h) as 100%. *$p < 0.05$, analysis of variance, as compared with vehicle treatment.

treatment for 2 days. Although the viability of the cells was 100% in both vehicle- and indomethacin-treated cells as shown by dotted lines in the right *Y*-axis of Fig. 4C, the indomethacin-treated cells were alive but not growing. In addition, growth inhibition was also observed in the cells treated with the same concentrations of aspirin, diclofenac and sulindac as used for Fig. 2 (data not shown). Thus, the increase in migration and scattered spreading of indomethacin-treated cells may not have been due to a simple increase in cell growth as shown in the control cells.

3.4. Indomethacin reduces E-cadherin expression in A549 cells

As shown in Fig. 4, the indomethacin-treated A549 cells were discretely spread out, which is to say, were dissociated from the connected epithelial cell aggregates and migrated individually. Therefore, expression of one of the major adhesion molecules, E-cadherin, was examined when the cells were treated with indomethacin since E-cadherin is known to play an important role in the maintenance of cell integrity [8]. For these experiments, A549 cells were treated with indomethacin for periods ranging from 2 h to 16 h and then the particulate fraction including membranes was collected and examined by western blotting. As shown in Fig. 5A, there was high basal expression of E-cadherin at time 0. However, treatment with indomethacin induced a time-dependent decrease in the expression of E-cadherin that started at 2 h and remained for 16 h. To ensure the equal loading of proteins, the blot shown in the upper panel of Fig. 5A was stripped and re-probed with antibodies to EGFR since A549 cells were reported to express EGFR endogenously [30]. As shown in the lower panel, nearly identical amounts of EGFR were present throughout the treatment.

3.5. Indomethacin reduces collagen IV expression in A549 cells

Many epithelial cells including A549 cells attach to culture dishes via a layer of extracellular matrix like the basal lamina. One of the components of the basal lamina is type IV collagen secreted by the epithelial cells [10]. Thus, the expression of collagen IV was examined when the cells were treated with indomethacin. Like the expression of E-cadherin shown in Fig. 5A, there was a high basal level of collagen IV at time 0 and treatment of the A549 cells with indomethacin induced a time-dependent decrease in the expression from 8 h to 16 h, without a change in β-tubulin levels, as shown in Fig. 5B.

3.6. Indomethacin activates matrix metalloproteinase-9 in A549 cells

Collagen IV is known to be degraded by a type IV collagenase called matrix metalloproteinase (MMP)-9, a.k.a. 92-kDa gelatinase or gelatinase B, and/or MMP-2 (gelatinase A) [9,10]. Thus, the enzymatic activity of MMPs was examined by the gelatin zymography assay when the cells were treated with indomethacin for 2–16 h. As shown in Fig. 6A, treatment with 300 μM indomethacin significantly increased the 92-kDa MMP-9 activity from 8 h corresponding to the decrease in expression of collagen IV, as shown in Fig. 5B. To confirm that the activity of MMP-9 was regulated by indomethacin, we used concentrations of indomethacin ranging from 3 μM to 300 μM for 8 h. As shown in Fig. 6B, a dose-dependent increase in the activity of MMP-9 was seen from 30 μM with a maximum at 100–300 μM. The dose-dependent effects of indomethacin were also seen in cellular morphological changes as shown in Fig. 6C, parallel to the activity of MMP-9 shown in Fig. 6B. In addition, the activity of MMP-2 was not detected in our experiments probably because the expression of MMP-2 was suppressed by treatment of A549 cells with indomethacin as previously reported [31].

3.7. Indomethacin-altered E-cadherin and collagen IV expression as well as matrix metalloproteinase-9 activity are restored by a peroxisome proliferator-activated receptor γ agonist, troglitazone

Besides the COX inhibition, indomethacin has been reported to regulate the activation of peroxisome proliferator-activated receptor (PPAR)γ [32,33]. Thus, we previously showed that treatment with a PPARγ agonist, troglitazone, restored the indomethacin-reduced expression of fatty acid translocase/CD36 in LS174T human colon cancer cells [34]. Therefore, we then examined the effect of troglitazone to verify if the effects of indomethacin on E-cadherin and collagen IV expression, as well as MMP-9 activation, were due to the altered activity of PPARγ in A549 cells. For these experiments, A549 cells were treated with indomethacin for 8 h following pretreatment with 10 μM trogli-

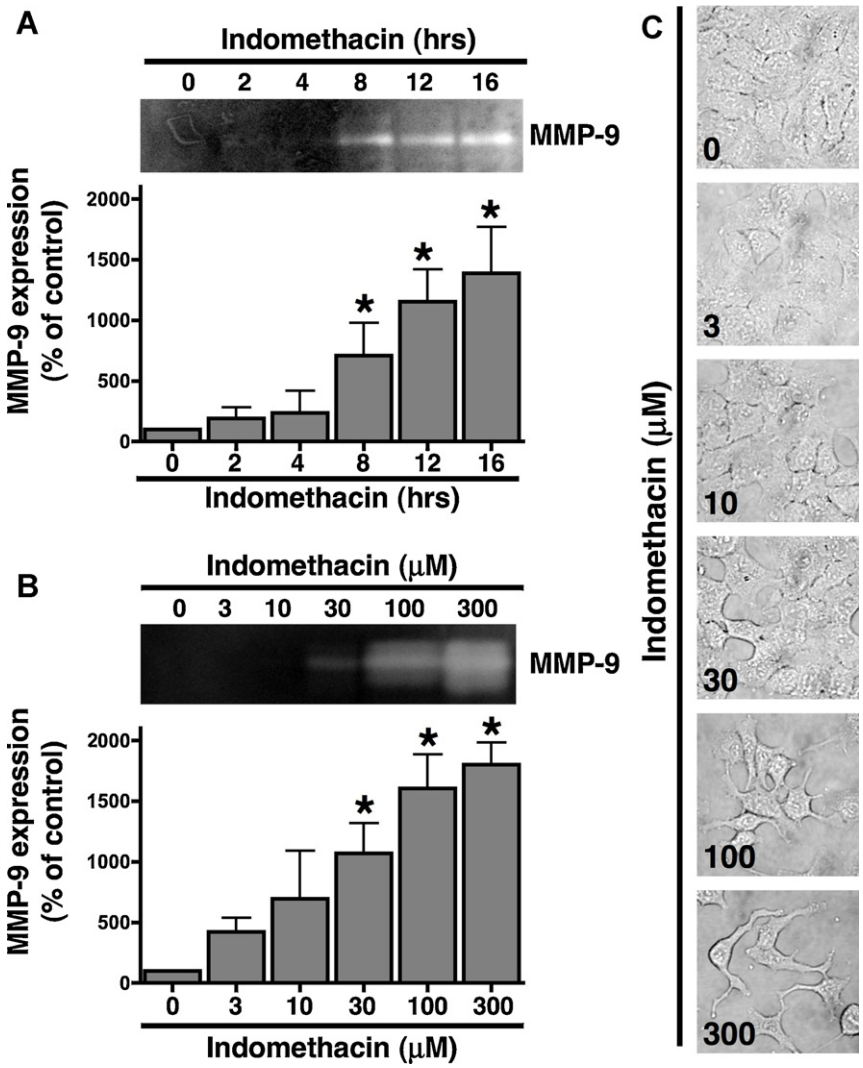

Fig. 6. Effects of indomethacin on MMP-9 activation. A: A549 cells were treated with vehicle or 300 μM indomethacin for the periods indicated. B: A549 cells were treated with vehicle or 3–300 μM indomethacin for 16 h. The cell culture medium was then collected and proteins including MMP-9 were precipitated using TCA and acetone and subjected to gelatin zymography as described under Section 2. The histogram represents the gelatin-degrading activity of MMP-9 as assessed with pooled densitometric data (mean ± S.D.) from three independent experiments. Data are normalized to the vehicle-treated controls (0 h (A) or 0 μM (B)) as 100%. $^{*}p < 0.05$, analysis of variance, as compared with vehicle treatment. C: A549 cells were treated with vehicle or 3–300 μM indomethacin for 16 h. Images under visible light were obtained as described under Section 2. The results are representative of more than three independent experiments.

tazone for 15 min and then assays were performed in similar ways to those for Figs. 5 and 6. As shown in Fig. 7A and B, the indomethacin-mediated expression of E-cadherin and collagen IV recovered significantly when the cells were pretreated with 10 μM troglitazone for 15 min. Correspondingly, indomethacin-mediated MMP-9 activation was significantly reduced by pretreatment with 10 μM troglitazone for 15 min as shown in Fig. 7C. In addition, although it was very slight, A549 cells expressed PPARγ endogenously as reported previously [35], and the levels of expression were not altered following treatment of the cells with up to 300 μM indomethacin for at least 16 h (data not shown). These results indicate that the expression of E-cadherin and collagen IV as well as activation of MMP-9 by indomethacin was regulated by the activity of PPARγ in A549 cells.

3.8. Indomethacin-altered cellular morphological changes and migration are restored by a peroxisome proliferator-activated receptor γ agonist, troglitazone

Finally, we further confirmed whether restoration of the expression of E-cadherin and collagen IV, as well as the inactivation of MMP-9 by pretreatment with troglitazone, really sets off the changes in cellular morphology induced by indomethacin in A549 cells. For these experiments, A549 cells were treated with indomethacin for 24 h following pretreatment with 10 μM troglitazone for 15 min and then assays were performed in a similar fashion to those in Figs. 3 and 4B. As shown in the lower panels in Fig. 8A, in the phalloidin-stained A549 cells, pretreatment with troglitazone prior to treatment with indomethacin caused a loss of stress fibers to some extent; however, it had appreciable effects on the cellular morphological changes. Thus, a number of indomethacin-treated A549 cells were considerably less shrunken and elongated following pretreatment with troglitazone. Interestingly, treatment with troglitazone itself for 24 h caused a slight dissociation of the cells in both vehicle- and indomethacin-treated cells. As shown in Fig. 8B, treatment with troglitazone itself induced considerable migration among A549 cells. However, although it was not completely blocked, indomethacin-treatment-related migration was significantly reduced by troglitazone pretreatment. These results strongly indicate that PPARγ is one of the key regulators of cellular migration and cellular morphological changes induced by indomethacin in A549 cells.

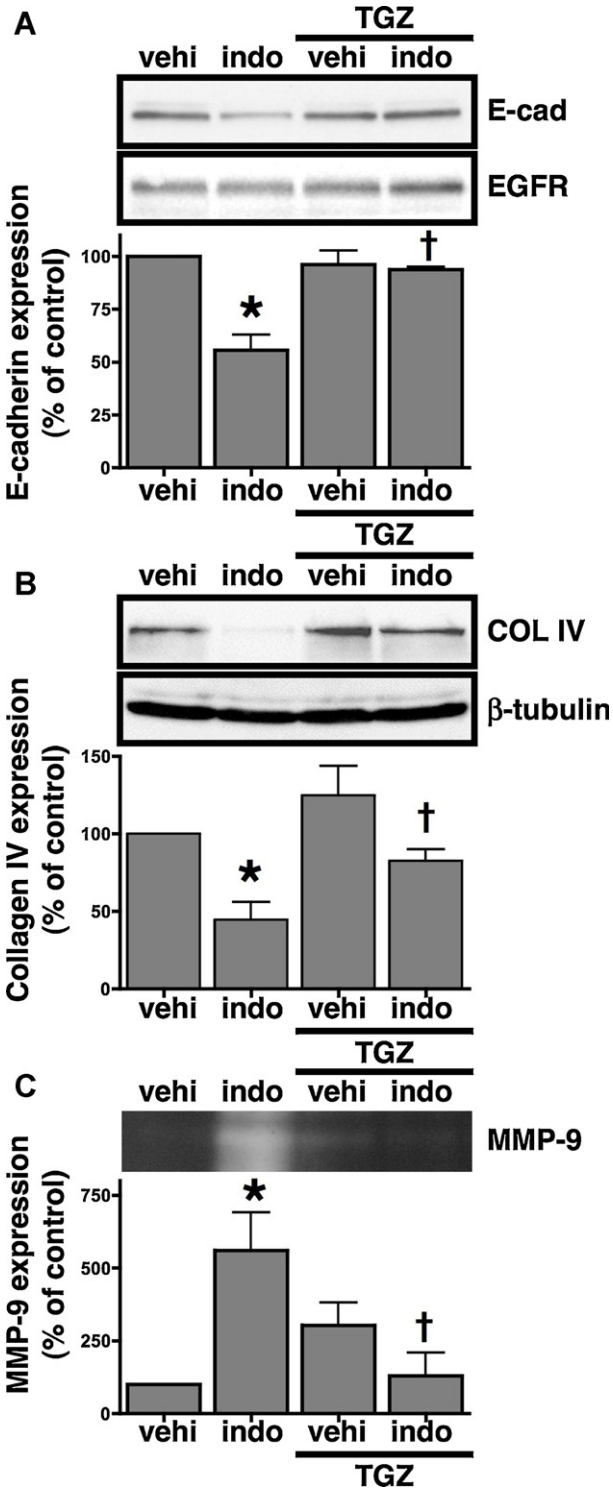

Fig. 7. Effects of troglitazone (TGZ) on indomethacin-induced expression of E-cadherin (A) and collagen IV (B), and activation of MMP-9 (C). A549 cells were pretreated with vehicle or 10 μM TGZ for 15 min then treated with vehicle or 300 μM indomethacin for 8 h. A: A particulate (membrane) fraction was prepared as described under Section 2 and subjected to immunoblot analysis for E-cadherin (E-cad, upper panel) and EGF receptors (EGFR, lower panel). A representative immunoblot is shown. The histogram represents the ratio of E-cadherin to EGFR as assessed with pooled densitometric data (mean ± S.D.) from three independent experiments. B: Upper panel: immunoblotting with antibodies against collagen IV (COL IV). Lower panel: immunoblotting with antibodies against β-tubulin. The histogram represents the ratio of collagen IV to β-tubulin as assessed with pooled densitometric data (mean ± S.D.) from three independent experiments. C: The cell culture medium was then collected and proteins including MMP-9 were subjected to gelatin zymography. The histogram represents the gelatin-degrading activity of MMP-9 as assessed with pooled densitometric data (mean ± S.D.) from three independent experiments. Data are normalized to the vehicle-treated controls as 100%. $^{*}p < 0.05$, *t*-test, as compared with vehicle treatment. $\dagger p < 0.05$, *t*-test, as compared with indomethacin treatment.

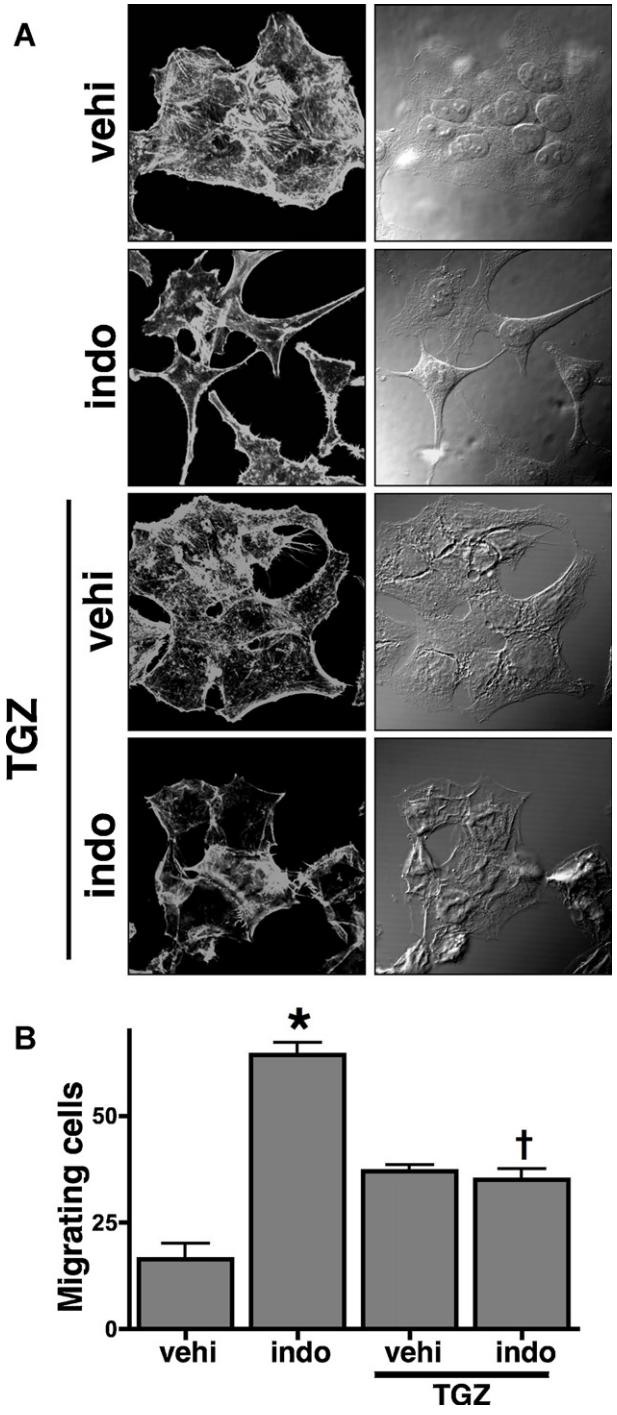

Fig. 8. Effect of troglitazone (TGZ) on indomethacin-induced changes in actin stress fibers and cellular morphology (A), and on cell migration in a transwell filter assay (B). A549 cells were pretreated with vehicle or 10 μM TGZ for 15 min then treated with vehicle or 300 μM indomethacin for 24 h. A: Cells were fixed and stained with TRITC-phalloidin to examine changes in the formation of stress fibers. Images were obtained as described under Section 2. Left panels: images of TRITC-phalloidin-stained stress fibers in indomethacin-treated A549 cells. Right panels: the same fields photographed under visible light. The results are representative of more than three independent experiments. B: A549 cells in upper chamber were treated with vehicle or 300 μM indomethacin for 24 h. The cells that migrated to the bottom chamber were trypsinized and then counted. The histogram represents the migrating cells (mean ± S.E.M.) from three independent experiments. $^{*}p < 0.05$, *t*-test, as compared with vehicle treatment. $\dagger p < 0.05$, *t*-test, as compared with indomethacin treatment.

4. Discussion

4.1. Indomethacin presumably regulates the malignancy of cancer cells by epithelial-mesenchymal transition and mesenchymal-epithelial transition in A549 cells

Indomethacin, a potent NSAID, is reported to have anti-proliferative and pro-apoptotic effects on mouse tumor cells in vitro and on mice in vivo [36], as well as on human cancer cell lines including A549 cells [37]. The prominent effects provoked by indomethacin in A549 cells, such as losses of stress fibers, E-cadherin, and collagen IV as shown in Fig. 5, and increased activation of MMP-9 as shown in Fig. 6, are features of the complex reprogramming of epithelial cells known as EMT. As described in Section 1.1 of the Introduction, EMT is characterized as a process that plays essential roles in development and enhanced cell migration for wound healing [12,38]. However, if aberrant wound repair processes occur in cancer cells, EMT may lead to cancer cell migration and invasion known as metastasis. Interestingly, indomethacin-induced EMT was reversible when the cells were washed to remove indomethacin (data not shown). The reverse of EMT is referred to as mesenchymal-epithelial transition (MET) [6]. In terms of the wound healing process, MET is considered essential for re-establishing the barrier function by re-expression of E-cadherin and other epithelial markers when wound repair is underway. Thus, after facilitating cellular migration to the site of injury by EMT, cells should gain the ability to proliferate for complete wound closure possibly via MET [12]. Therefore, in the case of indomethacin treatment, the cancer cells may start growing because of MET, if indomethacin is removed from the cells during the migration, for instance, by washing out and/or dissociation in the bloodstream. The reversible effects of indomethacin on EMT and MET plausibly set up the cancer malignancy via a two-step process. The first step evoked by indomethacin-induced EMT causes the physical translocation of the cancer cells to distant tissues and/or organs, whereas the second step evoked by removal of indomethacin at distal sites involves the development of malignant lesions by the cancer cells developing proliferative activity by MET.

4.2. Peroxisome proliferator-activated receptor γ is implicated in indomethacin-induced epithelial-mesenchymal transition in A549 cells

In addition to inhibiting COX as an NSAID, indomethacin is reported to regulate the activation of PPARγ as an agonist [32] or antagonist [33]. Generally, PPARγ ligands are reported to have inhibitory effects on many processes including proliferation and metastasis in lung cancer cells [39]. Treatment of A549 cells with troglitazone enhanced the transcriptional activity of PPARγ and induced dose-dependent inhibition of cell proliferation without the induction of apoptosis [35]. The same group also showed that treatment with troglitazone prevented metastasis by inhibiting EMT in A549 cells [40]. Moreover, in murine macrophages, treatment with troglitazone abrogated the expression of MMP-9 [41]. Indeed, the indomethacin-affected expression of E-cadherin and collagen IV was restored by the pretreatment with troglitazone as shown in Fig. 7A and B. The indomethacin-induced activation of MMP-9 was also inhibited by the troglitazone pretreatment as shown in Fig. 7C, accompanied by reductions in the cellular morphological changes as well as migration of the A549 cells as shown in Fig. 8, suggesting an inhibitory effect of troglitazone on indomethacin-induced EMT in A549 cells. Although pretreatment with troglitazone significantly reduced indomethacin-induced EMT in A549 cells, morphological changes and migration were not blocked completely. Indeed, treatment with troglitazone itself

slightly evoked the activation of MMP-9 and cellular migration, as shown in Figs. 7C and 8B, respectively. Taking these findings together, indomethacin presumably activates PPARγ as an agonist, which eventually leads to reduced activation of PPARγ, since over-activation of PPARγ by an agonist is reported to down-regulate the expression of PPARγ protein and DNA-binding activity as a negative feedback loop [42]. Thus, as we discussed previously [34], because of its high affinity, troglitazone binds to PPARγ more competitively than indomethacin and activates PPARγ. However, troglitazone may not over-activate PPARγ followed by down-regulation of PPARγ expression because of its low efficacy. Therefore, troglitazone acted as a suppressive competitor for indomethacin [34]. As mentioned in Section 3.7 of the Results, the levels of endogenously expressed PPARγ in A549 cells were not altered following treatment with indomethacin (data not shown). Indomethacin may down-regulate not the expression of PPARγ protein but rather the DNA-binding activity. However, troglitazone is reported to activate not only PPARγ as an agonist but also PPARγ-independent multiple signaling pathways [43]. Thus, it is possible that the indomethacin-induced effects act in a PPARγ-independent manner, since diclofenac and sulindac are reported to act as an antagonist [44] and as an agonist [45] of PPARγ, respectively.

4.3. Is indomethacin-induced epithelial-mesenchymal transition only seen in lung cancer cells?

The use of NSAIDs is reported to be associated with a decreased risk of and/or protection against lung cancer by inhibiting cell growth [20]. Although the involvement of the COX-2/PGE_2 pathway is well studied, the effects of NSAIDs on lung cancer have been controversial, as described in Section 1.2 of the Introduction. Previous studies bundled individual NSAIDs, such as indomethacin, together. Therefore, it will be important to provide information on each NSAID individually because there is no widely accepted and effective strategy for preventing death from lung cancer, including information on the mechanism of metastasis. We here show the additional effect of indomethacin on cellular migration in NSCLC human A549 cells, which possibly enhances lung cancer malignancy owing to the induction of cellular metastasis. Although, using human colon cancer cell lines, the effects of indomethacin on inhibition of the uptake of a substrate for PGE_2, arachidonic acid, and reduction in expression of the EP2 subtype of PGE_2 receptor were shown as additional COX-independent anti-cancer effects [34,46,47], indomethacin-induced EMT has not been observed in LS174T and HCA-7 human colon cancer cells or in HepG2 and HuH7 human liver cancer cells (data not shown). Moreover, treatment of human breast cancer cells with indomethacin led to a less malignant phenotype and indeed reduced the invasiveness of the cells [48]. Thus, whether the additional effect of indomethacin on metastasis found in the present study only occurs in lung cancer needs to be examined. Although regular use of NSAIDs including indomethacin has been associated with a reduction in the risk of lung cancer by some epidemiological studies [21], the present study may provide a rational explanation, to some extent, for the difficulty in using indomethacin as an NSAID for lung cancer therapy. Thus, indomethacin has contrasting effects on NSCLC, inhibiting cellular growth but enhancing cancer cell migration/metastasis.

Acknowledgement

This research was supported in part by a Grant-in-Aid for Scientific Research (22590079) from the Ministry of Education, Culture, Sports, Science and Technology.

References

[1] Ulrich CM, Bigler J, Potter JD. Non-steroidal anti-inflammatory drugs for cancer prevention: promise, perils and pharmacogenetics. Nat Rev Cancer 2006;6:130–40.
[2] Cuzick J, Otto F, Baron JA, Brown PH, Bum J, Greenwald P, et al. Aspirin and non-steroidal anti-inflammatory drugs for cancer prevention: an international consensus statement. Lancet Oncol 2009;10:501–7.
[3] Wang MT, Honn KV, Nie D. Cyclooxygenases, prostanoids, and tumor progression. Cancer Metastasis Rev 2007;26:525–34.
[4] Chaffer CL, Weinberg RA. A perspective on cancer cell metastasis. Science 2011;331:1559–64.
[5] Potenta S, Zeisberg E, Kalluri R. The role of endothelial-to-mesenchymal transition in cancer progression. Br J Cancer 2008;99:1375–9.
[6] Thiery JP, Acloque H, Huang RYJ, Nieto MA. Epithelial-mesenchymal transitions in development and disease. Cell 2009;139:871–90.
[7] Peinado H, Olmeda D, Cano A. Snail ZEB and bHLH factors in tumour progression: an alliance against the epithelial phenotype? Nat Rev Cancer 2007;7:415–28.
[8] Bremnes RM, Veve R, Hirsch FR, Franklin WA. The E-cadherin cell-cell adhesion complex and lung cancer invasion, metastasis, and prognosis. Lung Cancer 2002;36:115–24.
[9] Chakrabarti S, Patel KD. Matrix metalloproteinase-2 (MMP-2) and MMP-9 in pulmonary pathology. Exp Lung Res 2005;31:599–621.
[10] Khoshnoodi J, Pedchenko V, Hudson BG. Mammalian collagen IV. Microsc Res Tech 2008;71:357–70.
[11] Muroski ME, Roycik MD, Newcomer RG, Van den Steen PE, Opdenakker G, Monroe HR, et al. Matrix metalloproteinases-9/gelatinase B is a putative therapeutic target of chronic obstructive pulmonary disease and multiple sclerosis. Curr Pharm Biotechnol 2008;9:34–46.
[12] McConkey DJ, Choi W, Marquis L, Martin F, Williams MB, Shah J, et al. Roles of epithelial-to-mesenchymal transition (EMT) in drug sensitivity and metastasis in bladder cancer. Cancer Metastasis Rev 2009;28:335–44.
[13] Hazan RB, Qiao R, Keren R, Badano I, Suyama K. Cadherin switch in tumor progression. Ann N Y Acad Sci 2004;1014:155–63.
[14] Cataldo VD, Gibbons DL, Perez-Soler R, Quintas-Cardama A. Treatment of non-small-cell lung cancer with erlotinib or gefitinib. N Engl J Med 2011;364:947–55.
[15] Galetta D, Rossi A, Pisconti S, Millaku A, Colucci G. Maintenance or non-maintenance therapy in the treatment of advanced non-small cell lung cancer: that is the question. Cancer Treat Rev 2010;36S3:S30–3.
[16] Taimur S, Edelman MJ. Treatment options for brain metastases in patients with non-small-cell lung cancer. Curr Oncol Rep 2003;5:342–6.
[17] Schuette W. Treatment of brain metastases from lung cancer: chemotherapy. Lung Cancer 2004;45:S253–7.
[18] Yamanaka R. Medical management of brain metastases from lung cancer (Review). Oncol Rep 2009;22:1269–76.
[19] Horn L, Backlund M, Johnson DH. Targeting the eicosanoid pathway in non-small-cell lung cancer. Expert Opin Ther Targets 2009;13:675–88.
[20] Krysan K, Reckamp KL, Sharma S, Dubinett SM. The potential and rationale for COX-2 inhibitors in lung cancer. Anticancer Agents Med Chem 2006;6:209–20.
[21] Brown JR, DuBois RN. Cyclooxygenase as a target in lung cancer. Clin Cancer Res 2004;10:4266s–9.
[22] Wall RJ, Shyr Y, Smalley W. Nonsteroidal anti-inflammaatory drugs and lung cancer risk: a population-based case control study. J Thorac Oncol 2007;2:109–14.
[23] Hayes JH, Anderson KE, Folsom AR. Association between nonsteroidal anti-inflammatory drug use and the incidence of lung cancer in the Iowa women's health study. Cancer Epidemol Biomarkers Prev 2006;15:2226–31.
[24] Fujino H, Pierce KL, Srinivasan D, Protzman CE, Krauss AH, Woodward DF, et al. Delayed reversal of shape change in cells expressing FP_B prostanoid receptors. Possible role of receptor resensitization. J Biol Chem 2000;275:29907–14.
[25] Fujino H, Toyomura K, Chen XB, Regan JW, Murayama T. Prostaglandin E_2 regulates cellular migration via induction of vascular endothelial growth factor receptor-1 in HCA-7 human colon cancer cells. Biochem Pharmacol 2011;81:379–87.
[26] Fujino H, Srinivasan D, Regan JW. Cellular conditioning and activation of β-catenin signaling by the FP_B prostanoid receptor. J Biol Chem 2002;277:48786–95.
[27] Hanaka H, Pawelzik SC, Johnsen JI, Rakonjac M, Terawaki K, Rasmuson A, et al. Microsomal prostaglandin E synthase 1 determines tumor growth in vivo of prostate and lung cancer cells. Proc Natl Acad Sci USA 2009;106:18757–62.
[28] Jordan MA, Wilson L. Microtubules and actin filaments: dynamic target for cancer chemotherapy. Curr Opin Cell Biol 1988;10:123–30.
[29] Gialeli D, Theocharis AD, Karamanos NK. Roles of matrix metalloproteinases in cancer progression and their pharmacological targeting. FEBS J 2011;278:16–27.
[30] Al-Nedawi K, Meehan B, Kerbel RS, Allison AC, Rak J. Endotherial expression of autocrine VEGF upon the uptake of tumor-derived microvesicles containing oncogenic EGFR. Proc Natl Acad Sci USA 2009;106:3794–9.
[31] Pan MP, Chuang LY, Hung WC. Non-steroidal anti-inflammatory drugs inhibit matrix metalloproteinase-2 expression via repression of transcription in lung cancer cells. FEBS Lett 2001;508:365–8.
[32] Lehmann JM, Lenhard JM, Oliver BB, Ringold GM, Kliewer SA. Peroxisome proliferator-activated receptors α and γ are activated by indomethacin and other non-steroidal anti-inflammatory drugs. J Biol Chem 1997;272:3406–10.

[33] Bishop-Bailey D, Warner TD. PPARγ ligands induce prostaglandin production in vascular smooth muscle cells: indomethacin acts as a peroxisome proliferator-activated receptor-γ antagonist. FASEB J 2003;17:1925–7.
[34] Orido T, Fujino H, Kawashima T, Murayama T. Decrease in uptake of arachidonic acid by indomethacin in LS174T human colon cancer cells; a novel cyclooxygenase-2-inhibition-independent effect. Arch Biochem Biophys 2010;494:78–85.
[35] Keshamouni VG, Reddy RC, Arenberg DA, Joel B, Thannickal VJ, Kalemkerian GP, et al. Peroxisome proliferator-activated receptor-γ activation inhibits tumor progression in non-small-cell lung cancer. Oncogene 2004;23: 100–8.
[36] Eli Y, Przedecki F, Levin G, Kariv N, Raz A. Comparative effects of indomethacin on cell proliferation and cell cycle progression in tumor cells grown in vitro and in vivo. Biochem Pharmacol 2001;61:565–71.
[37] Sharma SD, Meeran SM, Katiyar SK. Proanthocyanidins inhibit in vitro and in vivo growth of human non-small cell lung cancer cells by inhibiting the prostaglanidn E_2 and prostaglandin E_2 receptors. Mol Cancer Ther 2010;9: 569–80.
[38] Crosby LM, Waters CM. Epitherial repair mechanisms in the lung. Am J Physiol Lung Cell Mol Physiol 2010;298:L715–31.
[39] Reka AK, Goswami MT, Krishnapuram R, Standiford TJ, Keshamouni VG. Molecular cross-regulation between PPAR-γ and other signaling pathways: implications for lung cancer therapy. Lung Cancer 2011;72:154–9.
[40] Reka AK, Kurapati H, Narala VR, Bommer G, Chen J, Standiford TJ, et al. Peroxisome proliferator-activated receptor-γ activation inhibits tumor metastasis by antagonizing Smad3-mediated epithelial-mesenchymal transition. Mol Cancer Ther 2010;9:3221–32.
[41] Ricote M, Li AC, Willson TM, Kelly CJ, Glass CK. The peroxisome proliferator-activated receptor-γ is a negative regulator of macrophage activation. Nature 1998;391:79–82.
[42] Camp HS, Whitton AL, Tafuri SR. PPARγ activators down-regulate the expression of PPAR(in 3T3-L1 adipocytes. FEBS Lett 1999;447:186–90.
[43] Wei S, Yang J, Lee SL, Kulp SK, Chen CS. PPARγ-independent antitumor effects of thiazolidinediones. Cancer Lett 2009;276:119–24.
[44] Adamson DJA, Frew D, Tatoud R, Wolf R, Palmer CAN. Diclofenac antagonizes peroxisome proliferator-activated receptor-γ signaling. Mol Pharmacol 2002;61:7–12.
[45] Wick M, Hurteau G, Dessev C, Chan D, Geraci MW, Winn RA, et al. Peroxisome proliferator-activated receptor-γ is a target of nonsteroidal anti-inflammatory drugs mediating cyclooxygenase-independent inhibition of lung cancer cell growth. Mol Pharmacol 2002;62:1207–14.
[46] Fujino H, Chen XB, Regan JW, Murayama T. Indomethacin decreases EP2 prostanoid receptor expression in colon cancer cells. Biochem Biophys Res Commun 2007;359:568–73.
[47] Orido T, Fujino H, Toyomura K, Kawashima T, Murayama T. Indomethacin decreases arachidonic acid uptake in HCA-7 human colon cancer cells. J Pharmacol Sci 2008;108:389–92.
[48] Glunde K, Jie C, Bhujwalla ZM. Mechanisms of indomethacin-induced alterations in the choline phospholipids metabolism of brest cancer cells. Neoplasia 2006;8:758–71.